Evolutionarily conserved glycan signal to degrade aberrant brassinosteroid receptors in *Arabidopsis*

Zhi Hong[a,b,1], Hiroyuki Kajiura[c], Wei Su[a,2], Hua Jin[a,3], Akihisa Kimura[a], Kazuhito Fujiyama[c], and Jianming Li[a,1]

[a]Department of Molecular, Cellular, and Developmental Biology, University of Michigan, Ann Arbor, MI 48109; [b]State Key Laboratory of Pharmaceutical Biotechnology, School of Life Sciences, Nanjing University, Nanjing, 210093, China; and [c]International Center for Biotechnology, Osaka University, Osaka 565, Japan

Edited* by Joanne Chory, The Salk Institute for Biological Studies and Howard Hughes Medical Institute, La Jolla, CA, and approved May 28, 2012 (received for review November 21, 2011)

Asparagine-linked glycans (N-glycans) are crucial signals for protein folding, quality control, and endoplasmic reticulum (ER)-associated degradation (ERAD) in yeast and mammals. Although similar ERAD processes were reported in plants, little is known about their biochemical mechanisms, especially their relationships with N-glycans. Here, we show that a missense mutation in the *Arabidopsis EMS-mutagenized bri1 suppressor 3* (*EBS3*) gene suppresses a dwarf mutant, *bri1-9,* the phenotypes of which are caused by ER retention and ERAD of a brassinosteroid receptor, BRASSINOSTEROID-INSENSITIVE 1 (BR1). *EBS3* encodes the *Arabidopsis* ortholog of the yeast asparagine-linked glycosylation 9 (ALG9), which catalyzes the ER luminal addition of two terminal α1,2 mannose (Man) residues in assembling the three-branched N-glycan precursor [glucose(Glc)]$_3$(Man)$_9$[*N*-acetylglucosamine(GlcNAc)]$_2$. Consistent with recent discoveries revealing the importance of the Glc$_3$Man$_9$GlcNAc$_2$ C-branch in generating an ERAD signal, the *ebs3-1* mutation prevents the Glc$_3$Man$_9$GlcNAc$_2$ assembly and inhibits the ERAD of bri1-9. By contrast, overexpression of *EBS4* in *ebs3-1 bri1-9,* which encodes the *Arabidopsis* ortholog of the yeast ALG12 catalyzing the ER luminal α1,6 Man addition, adds an α1,6 Man to the truncated N-glycan precursor accumulated in *ebs3-1 bri1-9,* promotes the bri1-9 ERAD, and neutralizes the *ebs3-1* suppressor phenotype. Furthermore, a transfer (T)-DNA insertional *alg3-T2* mutation, which causes accumulation of an even smaller N-glycan precursor carrying a different exposed α1,6 Man, promotes the ERAD of bri1-9 and enhances its dwarfism. Taken together, our results strongly suggest that the glycan signal to mark an ERAD client in *Arabidopsis* is likely conserved to be an α1,6 Man-exposed N-glycan.

Asparagine (Asn or *N*)-linked glycosylation is an important protein-modification process in all three domains of life (1). In animals, fungi, and plants, N-glycan is formed by transfer of a preassembled tetradecasaccharide Glc$_3$Man$_9$GlcNAc$_2$ (where Glc, Man, and GlcNAc represent glucose, mannose, and *N*-acetylglucosamine, respectively) from its lipid carrier, dolichyl-pyrophosphate (Dol-PP), to selective Asn residues on nascent polypeptides (2) (Fig. S1). The biosynthesis of the three-branched Glc$_3$Man$_9$GlcNAc$_2$ is a highly ordered assembly pathway at the endoplasmic reticulum (ER) membrane by sequential addition of sugars to the Dol-PP carrier involving highly specific glycosyltransferases that include ALG3, ALG9, and ALG12 catalyzing the ER luminal addition of an α1,3 Man, two α1,2 Man, and an α1,6 Man, respectively (Fig. S1) (3). The *N*-linked Glc$_3$Man$_9$GlcNAc$_2$ glycan is subsequently processed in the ER and Golgi by extensive deglycosylation and sugar additions.

Extensive studies in yeast and mammals revealed that ER-processed N-glycans serve as important signals for protein folding, quality control (QC), degradation, and sorting (4). Rapid sequential trimming of two Glc residues on the A-branch by glucosidase I (GI) and GII generates Glc$_1$Man$_9$GlcNAc$_2$, which interacts with calnexin (CNX) and its soluble homolog calreticulin (CRT), which recruit additional chaperones to facilitate protein folding, whereas removal of the last Glc by GII liberates glycoproteins from CNX/CRT (5) (Fig. S1). An incompletely/misfolded glycoprotein is recognized and reglucosylated by the ER-localized folding sensor UDP-Glc:glycoprotein glucosyltransferase (UGGT) for additional rounds of CNX/CRT-assisted folding, known as the CNX/CRT cycle (6). By contrast, slow trimming of the B-branch α1,2 Man by the ER α1,2 mannosidase I (ERManI) (7) (Fig. S1) was previously thought to create a critical N-glycan signal (Man$_8$GlcNAc$_2$) that interrupts futile CNX/CRT cycles of terminally misfolded proteins to deliver them for ER-associated degradation (ERAD) that involves retrotranslocation and cytosolic proteasomes (8). However, recent studies showed that whereas the B-branch α1,2 Man-trimming is a critical ERAD event, the actual N-glycan signal to mark an ERAD client is an exposed α1,6 Man generated by removing the terminal α1,2 Man from the C-branch (9, 10) (Fig. S1).

Although many studies reported the existence of similar ERQC and ERAD processes in plants (11, 12), little is known about their biochemical mechanisms, especially their relationship with N-glycan biosynthesis. Two *Arabidopsis* leucine-rich-repeat receptor-like kinases, BRASSINOSTEROID-INSENSITIVE 1 (BRI1) and EF-Tu Receptor (EFR), have recently emerged as model proteins to study ERQC and ERAD in plants (13). BRI1 functions as a cell surface receptor for the plant steroid hormone brassinosteroids (BRs) (14, 15), whereas EFR recognizes the bacterial translation elongation factor EF-Tu to initiate plant immunity responses (16). A Cys69Tyr mutation disrupting a highly conserved N-terminal disulfide bond and a Ser662Phe mutation in the BR-binding domain result in ER retention and ERAD of two structurally imperfect but biochemically competent BR receptors, bri1-5 and bri1-9, respectively, explaining their BR-insensitive dwarf phenotypes (17–19). A genetic screen looking for suppressors that restore the wild-type (WT) morphology to *bri1-9* led to identification of *EMS-mutagenized bri1 suppressor 1* (*EBS1*) and *EBS2*, encoding the *Arabidopsis* UGGT and a plant-specific CRT3, respectively (17, 18).

To identify additional factors of the plant ERQC and ERAD systems, we isolated and studied additional *ebs* mutants. We recently discovered that *EBS4* encodes the *Arabidopsis* ortholog of the yeast/human ALG12 that catalyzes the ER luminal addition of an α1,6 Man residue of Glc$_3$Man$_9$GlcNAc$_2$ and concluded that transfer of a completely assembled N-glycan precursor is required for successful ERAD of bri1-5 and bri1-9 (20).

Author contributions: Z.H. and J.L. designed research; Z.H., H.K., W.S., H.J., A.K., and K.F. performed research; H.K. and K.F. contributed new reagents/analytic tools; Z.H., H.K., W.S., H.J., K.F., and J.L. analyzed data; and Z.H. and J.L. wrote the paper.

The authors declare no conflict of interest.

*This Direct Submission article had a prearranged editor.

[1]To whom correspondence may be addressed. E-mail: zhihong@nju.edu.cn or jian@umich.edu.

[2]Present address: State Key Laboratory of Genetic Engineering and Institute of Plant Biology, School of Life Sciences, Fudan University, Shanghai 200433, China.

[3]Present address: Department of Biological Sciences, University of Illinois, Chicago, IL 60607.

This article contains supporting information online at www.pnas.org/lookup/suppl/doi:10.1073/pnas.1119173109/-/DCSupplemental.

Here, we report that the *Arabidopsis EBS3* gene encodes the *Arabidopsis* ortholog of the yeast/human ALG9 catalyzing the luminal addition of two α1,2 Man residues in assembling $Glc_3Man_9GlcNAc_2$ (21), further confirming our previous conclusion. Our studies using an *Arabidopsis alg3-T2* mutant that accumulates $Man_5GlcNAc_2$ (22, 23) and *EBS4*-overexpressing transgenic *ebs3-1 bri1-9* lines revealed that the glycan signal to mark ERAD clients in *Arabidopsis* is likely conserved to be an exposed α1,6 Man residue on N-glycans.

Results

***ebs3-1* Mutant Is Defective in the ERAD of bri1-9.** A previous genetic screen for extragenic suppressors of *bri1-9* isolated more than 80 *ebs* mutants, including *ebs1* and *ebs2* mutants defective in retaining bri1-9 in the ER (17, 18). A secondary screen looking for *ebs* mutants with increased bri1-9 abundance identified several potential ERAD mutants including *ebs3*, *ebs4* (20), and *ebs5* (24). As shown in Fig. 1*A*, both *ebs3-1* and *ebs4-1* accumulate more bri1-9 than *bri1-9*. To test if the increased bri1-9 abundance is caused by increased synthesis or reduced degradation, we treated 3-wk-old seedlings with cycloheximide (CHX), a widely used protein synthesis inhibitor, and analyzed the bri1-9 abundance by immunoblot. Fig. 1*B* shows that CHX caused a rapid disappearance of the mutant BR receptor in *bri1-9* but had a much weaker effect on the bri1-9 abundance in *ebs3-1 bri1-9*. A significant amount of bri1-9 was still present in *ebs3-1 bri1-9* 36 h after CHX treatment, whereas no bri1-9 was detectable after 12 h of CHX treatment in *bri1-9*. We, thus, concluded that the *ebs3-1* mutation inhibits the bri1-9 ERAD.

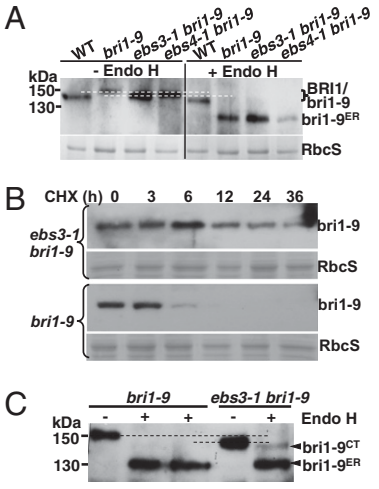

Fig. 1. *ebs3-1* mutation inhibits the ERAD of bri1-9. (*A*) Immunoblot analysis of bri1-9 in *ebs3-1 bri1-9*. (*B*) Immunoblot analysis of bri1-9 stability in *bri1-9* and *ebs3-1 bri1-9*. (*C*) Endo H analysis of bri1-9 in *bri1-9* and *ebs3-1 bri1-9*. For *A* and *C*, total proteins from 4-wk-old leaves were treated with or without Endo H, separated by SDS/PAGE, and analyzed by immunoblot with anti-BRI1 antibody. Equal amounts of total proteins were used in *A*, whereas five times more proteins in *bri1-9* than *ebs3-1 bri1-9* were used in *C*, which also contains technical duplicates of Endo H-treated *bri1-9* samples. For *B*, 3-wk-old seedlings were transferred from 1/2 MS-agar medium into liquid 1/2 MS medium containing 180 μM CHX. Equal amounts of seedlings were removed at different time points to extract total proteins into 2× SDS sample buffer, which were subsequently separated by SDS/PAGE and analyzed by immunoblot with anti-BRI1 antibody. The numbers on the left in *A* and *C* indicate molecular mass, bri1-9^{ER} denotes Endo H-sensitive form, and bri1-9^{CT} represents bri1-9 carrying C-type N-glycans. Dashed lines in *A* and *C* show the mobility difference between the bri1-9 band in *bri1-9* and that of *ebs3-1 bri1-9*. Coomassie blue staining of the small subunit of Rubisco (RbcS) serves as the loading control.

We also treated protein extracts with Endo H, an endoglycosidase that cleaves high-mannose-type (H-type) N-glycans of ER-localized proteins but cannot remove Golgi-processed complex-type (C-type) N-glycans (25). Fig. 1*A* shows that the vast majority of bri1-9 was Endo H-sensitive in *bri1-9* and two *ebs* mutants, indicating its predominant ER localization in all three genotypes. However, loading more proteins of *ebs3-1 bri1-9* detected a small amount of bri1-9 carrying C-type N-glycans indicative of ER escape, whereas increased loading failed to detect the C-type N-glycan-containing BR receptor in *bri1-9* (Fig. 1*C*). We suspected that the presence of a low level of the C-type N-glycan-containing bri1-9 in *ebs3-1 bri1-9*, likely attributable to saturation of the ER retention system by overaccumulated bri1-9 and its consequent leakage from the ER, is responsible for the suppressor phenotype because our earlier study showed that overexpression of bri1-9 could also suppress the *bri1-9* mutation (20). Consistently, expression of a genomic *EBS2* transgene, which encodes a rate-limiting factor for retaining bri1-9 in the ER (18, 24), neutralized the *ebs3-1* suppressive effect on *bri1-9* likely by preventing the ER leakage of a small amount of bri1-9 to the cell surface (Fig. S2).

***ebs3-1* Mutation Weakly Suppresses *bri1-9* with Partially Regained BR Sensitivity.** In line with accumulation of a low level of the C-type N-glycan–carrying bri1-9, *ebs3-1* is a weak suppressor of *bri1-9*. The rosette of *ebs3-1 bri1-9* is larger than that of *bri1-9* (Fig. 2*A*), and its etiolated hypocotyl and inflorescence stem are longer than those of *bri1-9* when grown in dark and soil, respectively (Fig. 2 *B* and *C*). The *ebs3-1* also weakly suppresses the *bri1-5* mutant that produces another ER-retained mutant BR receptor (19) (Fig. S3 *A* and *B*) but has no detectable effect on plant growth in a *BRI1*$^+$ background (Fig. S3*C*). As expected from the morphological and immunoblot analyses, *ebs3-1 bri1-9* partially regained BR sensitivity. Similar to what was previously reported (26), increasing concentrations of brassinolide (BL) (the most

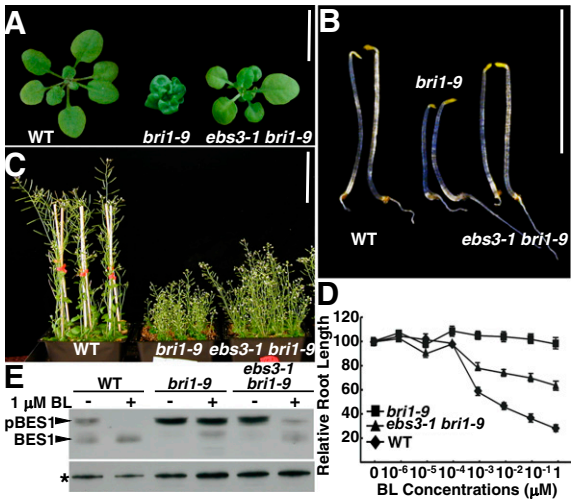

Fig. 2. *ebs3-1* is a weak suppressor of the *bri1-9* mutant. (*A*–*C*) Images of 3-wk-old soil-grown plants (*A*), 5-d-old etiolated seedlings (*B*), and 7-wk-old soil-grown mature plants (*C*) of WT, *bri1-9*, and *ebs3-1 bri1-9*. [Scale bars: 1 cm (*A* and *B*) and 10 cm (*C*).] (*D*) Quantitative analysis of BR sensitivity. Root length of 10-d-old seedlings grown on BL-containing medium were measured and presented as the relative value of average root length of BL-treated seedlings to that of mock-treated seedlings. Each data point represents the average of ~40 seedlings of duplicated experiments. Error bars denote SE. (*E*) Immunoblot analysis of BL-induced BES1 dephosphorylation. Total proteins were extracted in 2× SDS buffer from 2-wk-old seedlings treated with or without 1 μM BL for 1 h, separated by SDS/PAGE, and analyzed by immunoblot using an anti-BES1 antibody (27). Star indicates a nonspecific band for loading control.

active BR) had little effect on the root growth of *bri1-9* but inhibited that of the WT, as well as the *ebs3-1 bri1-9* mutant, albeit to a lesser extent (Fig. 2*D*). The regained BR sensitivity was also detected by immunoblot analysis of the BL-induced dephosphorylation of BRI1 EMS SUPPRESSOR1 (BES1), a very robust biochemical marker for BR signaling (27). Fig. 2*E* reveals that BL had little effect on the BES1 phosphorylation status in *bri1-9* but led to rapid dephosphorylation of BES1 in both the WT and *ebs3-1 bri1-9*.

***ebs3-1* Mutation Affects Assembly of the N-Glycan Precursor.** As indicated in Fig. 1 *A* and *C*, *ebs3-1* increases not only the abundance but also the electrophoretic mobility of bri1-9. Because the mobility of deglycosylated bri1-9 band of *ebs3-1 bri1-9* is the same as that of *bri1-9* (Fig. 1 *A* and *C*), the mobility difference of bri1-9 is attributable to different glycoforms of bri1-9 in the two mutants. The bri1-9 is either hypoglycosylated at fewer sites or fully glycosylated with smaller glycans. Because hypoglycosylation often leads to multiple isoforms of an affected glycoprotein each carrying different numbers of N-glycans (21), our detection of a single bri1-9 band in *ebs3-1 bri1-9* on immunoblot suggested that the observed mobility shift was caused by transfer of truncated N-glycan precursors to bri1-9. Further support for the presence of fully glycosylated bri1-9 with truncated glycans in *ebs3-1 bri1-9* came from our observation that no obvious mobility difference of the WT BRI1 was detected between the WT and the two *ebs* mutants (Fig. 3*A*). A hypoglycosylated BRI1 should move faster than a fully glycosylated BRI1 on protein gels, whereas a fully glycosylated BRI1 in WT, *ebs3-1*, and *ebs4-1* should exhibit the same mobility because BRI1 is not retained in the ER in all three genotypes and the *Arabidopsis* ER/Golgi-mediated glycan processing can effectively convert truncated H-type N-glycans, which are initially transferred in the ER to BRI1 in the two *ebs* mutants, to the same C-type N-glycans in the wild type (22, 23).

Further confirmation of a glycan-assembly defect came from size-fractionation (SF)-HPLC analysis of lipid-linked oligosaccharides (LLOs) of *bri1-9* and *ebs3-1 bri1-9*, which were fluorescently labeled with 2-pyridylamino (PA) following acidic hydrolysis of the Dol-PP linker. As shown in Fig. 3*B*, whereas *bri1-9* seedlings clearly accumulated the mature $Glc_3Man_9GlcNAc_2$ [with its PA-labeled derivative having an identical elution position with the $Glc_3Man_9GlcNAc_2$ (G3M9)-PA standard], the corresponding peak was absent in the *ebs3-1 bri1-9* sample. Instead, two major peaks comigrating with M5 and M6 standards were detected in *ebs3-1 bri1-9*. The identity of the M6 peak was determined by reverse-phase (RP)-HPLC as $Man_6GlcNAc_2^{ER}$, whereas the M5 peak was found to be a mixture of a small amount of $Man_5GlcNAc_2^{ER}$ and several minor contaminants (Fig. S4 *A* and *B*).

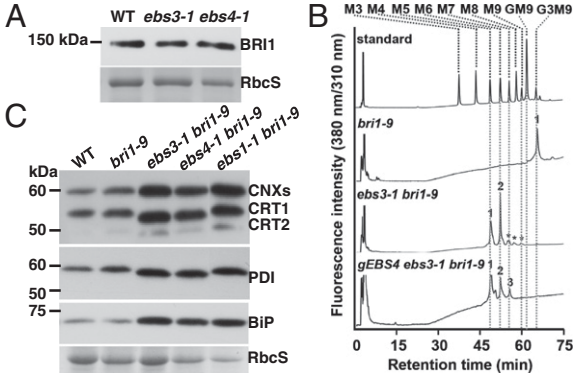

Fig. 3. *ebs3-1* likely affects assembly of the N-glycan precursor. (*A*) Immunoblot analysis of BRI1 in WT and *ebs3-1 BRI1*$^+$. (*B*) Analysis of LLOs in *bri1-9*, *ebs3-1 bri1-9*, and a transgenic *gEBS4 ebs3-1 bri1-9* line. LLOs of mature plants were extracted, acid-hydrolyzed, fluorescently labeled with PA, and analyzed using SF-HPLC by comparing their elution profiles with that of PA-sugar chain standards (Mn for $Man_nGlcNAc_2$-PA and G3M9 for $Glc_3Man_9GlcNAc_2$-PA). Asterisks indicate minor contaminants derived from the labeling process. (*C*) *ebs3-1* affects the electrophoretic mobility of several ER-localized glycoproteins. For *A* and *C*, equal amounts of total proteins from 4-wk-old leaves were separated by SDS/PAGE and analyzed by immunoblot with antibodies against BRI1, maize CRT, PDI, or BiP. Numbers on the left indicate molecular mass. Coomassie blue staining of RbcS served as a loading control.

The effect of *ebs3-1* on N-glycan assembly was also examined for several other ER-localized proteins, including a protein disulfide isomerase (PDI) (28), an ER-localized heat shock protein 70 (known as BiP) (29), and members of the CRT/CNX family (30). As shown in Fig. 3*C*, the mobility of PDI and CRT1 in *ebs3-1 bri1-9* is slightly faster than that in *bri1-9* and is similar to that in *ebs4-1* (20). Fig. 3*C* also shows that *ebs3-1* slightly activates the unfolded protein response (UPR), a master ER-surveillance system that stimulates synthesis of many ER chaperones in response to ER stresses (12). The protein abundance of CRTs, PDI, and BiP was slightly increased in *ebs3-1* compared with the WT and *bri1-9* and was similar to that in *ebs1-1* and *ebs4-1*.

Cloning of the *EBS3* Gene. Based on the effects of *ebs3-1* on the bri1-9 glycoforms and the LLO composition, we suspected that *EBS3* might encode another ER-localized mannosyltransferase. PCR-based molecular mapping (*SI Materials and Methods*) located the *EBS3* locus to a 200-kb region on the top of chromosome 1 that contains 59 annotated genes (Fig. S5 *A* and *B*). One of them, *At1g16900*, consisting of 10 exons and 9 introns (Fig. S5*C*), encodes a 570-aa protein highly similar to the yeast/human ALG9 (yALG9/hALG9) α1,2 mannosyltransferase and several predicted plant ALG9 homologs (Fig. S5*D*). The yALG9/hALG9 catalyzes the ER luminal addition of two α1,2 Man residues to assemble $Glc_3Man_9GlcNAc_2$ (Fig. S1), and mutations in yALG9 result in accumulation of the $Man_6GlcNAc_2^{ER}$ glycan and inhibition of ERAD in yeast (21, 31–34). Sequencing analysis of PCR-amplified *At1g16900* DNA from *ebs3-1 bri1-9* revealed a single-nucleotide change that mutates Arg100 to Trp (Fig. S5*D*). This Arg residue is located near the end of the largest luminal loop between the first two predicted transmembrane segments (Fig. S5 *D* and *E*) and is absolutely conserved in all known ALG9s and two other α1,2 mannosyltransferases, phosphatidylinositol glycan anchor biosynthesis class B protein (PIG-B) and SMP3, involved in glycosylphosphatidylinositol synthesis (35). A further proof for *At1g16900* being the *EBS3* gene came from our rescue experiment showing that a genomic *At1g16900* transgene rescued the morphological phenotype of *ebs3-1* (Fig. 4*A* and Fig. S6) and its N-glycan and ERAD defects of bri1-9 (Fig. 4*B*).

EBS3 Is the *Arabidopsis* Ortholog of yALG9. To directly test whether EBS3 is an ortholog of yALG9, we took advantage of the existence of a yeast *Δalg9 wbp1-2* double mutant that exhibits a temperature-sensitive growth phenotype (21). We replaced the ORF of *yALG9* in the *pYEp352-yALG9* expression plasmid with that of *EBS3* to generate *pYEp352-EBS3*, introduced the Arg100Trp mutation to make *pYEp352-ebs3-1*, and individually transformed the three plasmids and a vector control into the *Δalg9 wbp1-2* strain. As shown in Fig. 4*C*, transformation of the *yALG9* or *EBS3* plasmid but not the *ebs3-1* or vector plasmid suppressed the 33 °C growth defect of the *Δalg9 wbp1-2* mutant. We also transformed each plasmid into the *Δalg9* single mutant and analyzed the glycosylation pattern of vacuolar carboxypeptidase Y (CPY) carrying 4 glycosylation sites (36). As shown in Fig. 4*D*, both *yALG9* and *EBS3* but not the vector or *ebs3-1* plasmid rescued the glycosylation defect of CPY, converting three faster-moving hypoglycosylated CPY* bands into a single mature CPY band (mCPY) with identical mobility to that of WT cells. These results demonstrated that EBS3

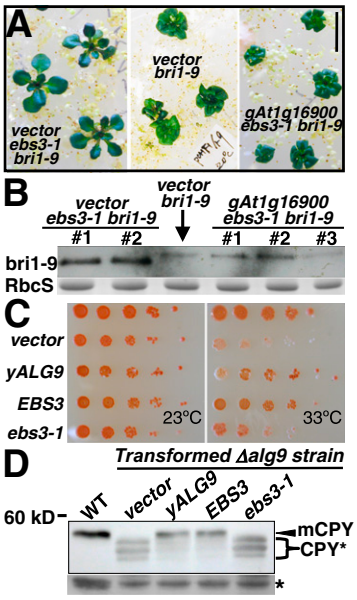

Fig. 4. *EBS3* encodes the *Arabidopsis* ortholog of yALG9. (*A*) Images of 3-wk-old transgenic *bri1-9* lines carrying an empty vector and transgenic *ebs3-1 bri1-9* seedlings carrying a genomic *EBS3* transgene (*gEBS3*) or an empty vector. (Scale bar: 1 cm.) (*B*) Immunoblot analysis of bri1-9. The numbers on top of the gel panel indicate different transgenic lines. (*C*) *EBS3* complemented the yeast *Δalg9* mutation. Growth efficiency of WT or *Δalg9 wbp1-2* cells transformed with the vector or an expression plasmid of *yALG9*, *EBS3* or *ebs3-1* cDNA. Transformants were spotted in 10-fold serial dilution on synthetic medium and grown for 3 d at 23 °C or 33 °C. (*D*) Immunoblot analysis of CPY of the WT yeast strain and *Δalg9* strain transformed with indicated plasmids. For *B* and *D*, equal amounts of total proteins extracted from 4-wk-old soil-grown seedlings (*B*) or yeast cells of midlog growth phase (*D*) were separated by SDS/PAGE and analyzed by immunoblot using an anti-BRI1 (*B*) or anti-CPY (*D*) antibody. Coomassie blue staining of RbcS served as a loading control in (*B*). mCPY indicates the mature CPY, CPY*s represent three isoforms of CPY carrying different numbers of truncated N-glycan in (*D*), and star denotes a cross-reacting band used for loading control.

is the *Arabidopsis* ortholog of yALG9 and that the Arg100Trp mutation destroys its α1,2 mannosyltransferase activity.

Exposed α1,6 Mannose Residue Is the Likely Glycan Signal for the bri1-9 ERAD. Recent studies revealed that the ERAD signal in yeast and mammals is an exposed α1,6 Man on N-glycans generated by removing an α1,2 Man residue from the C-branch (9, 10) (Fig. S1). This unique demannosylation was catalyzed by the yeast homologous to mannosidase I (Htm1) and its mammalian homologs, ER degradation enhancing-mannosidase-like proteins (EDEMs) (37). We hypothesized that the most likely reason for the defective bri1-9 ERAD in *ebs3-1 bri1-9* is lack of a correct ERAD glycan signal on bri1-9.

To test our hypothesis, we used a previously described genetic method for generating α1,6 Man-exposed N-glycans in *ebs3-1*. It was known that overexpressed yeast ALG12 could bypass the requirement of an intact B-branch for adding the second α1,6 Man to $Man_6GlcNAc_2^{ER}$ to generate a unique $Man_7GlcNAc_2$ glycan (38) (Fig. 5*A*). If an α1,6 Man-exposed N-glycan was the ERAD signal in *Arabidopsis*, we would expect that overexpression of *EBS4* (encoding the *Arabidopsis* ALG12) should suppress the *ebs3-1 bri1-9* phenotype and rescue the ERAD defect of bri1-9. Indeed, as shown in Fig. 5*B*, *gEBS4 ebs3-1 bri1-9* transgenic mutants were morphologically similar to or even smaller than a typical *EBS3*-rescued *ebs3-1 bri1-9* mutant. SF-HPLC analysis of LLOs of the *gEBS4 ebs3-1 bri1-9* transgenic plants revealed the presence of a small peak at the position of a M7 standard (Fig. 3*B*), which was determined by RP-HPLC to contain the predicted $Man_7GlcNAc_2$ B-isoform with an exposed α1,6 Man (Fig. S4*C*). Although $Man_6GlcNAc_2$ remains the major LLO in the *gEBS4 ebs3-1 bri1-9* line, a mere 7.14% (1/14) conversion efficiency of $Man_6GlcNAc_2^{ER}$ to $Man_7GlcNAc_2^{ER}$ is sufficient to have, on average, 1 α1,6 Man-exposing N-glycan on each bri1-9 (containing 14 predicted N-glycan sites) for marking the mutant receptor for ERAD. Indeed, an immunoblot analysis showed that *EBS4* overexpression could reverse the inhibitory effect of *ebs3-1* on the bri1-9 ERAD while causing little change in its mobility on protein gels (Fig. 5*C*).

Additional support for an α1,6 Man-exposed N-glycan being the critical ERAD signal came from our genetic analysis of an *Arabidopsis alg3* mutant. Loss-of-function *alg3* mutations block the formation of $Glc_3Man_6GlcNAc_2$, resulting in transfer of $Glc_3Man_5GlcNAc_2$ with a different free α1,6 Man from Dol-PP to proteins (Fig. 5*A*) (22, 23), whereas a recent study showed a normal ERAD process in an yeast *Δalg3* mutant (9). If this α1,6 Man can also function as an ERAD signal in *Arabidopsis*, we would expect that an *alg3* mutation should promote rather than inhibit the ERAD of bri1-9. We obtained a transfer (T)-DNA insertional *alg3* mutant [The Arabidopsis Information Resource (TAIR) accession no. SALK_046061; previously named *alg3-T2*] (39) and crossed the *alg3-T2* mutation into *bri1-9*. Fig. 5*D* shows that the *alg3-T2 bri1-9* mutant is morphologically more severe than *bri1-9*. It is important to note that *alg3-T2* itself has no detectable effect on plant growth (23), although it does activate UPR because the abundance of PDI in *alg3-T2 bri1-9* is significantly higher than that in *bri1-9* (Fig. 5*E*). By contrast, a T-DNA insertional mutation of the *Arabidopsis* stroma cell-derived factor

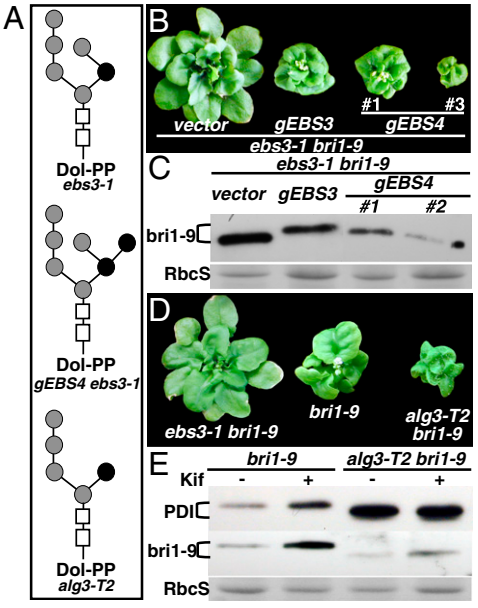

Fig. 5. An exposed α1,6 Man residue is likely the glycan signal for bri1-9 ERAD. (*A*) Schematic structures of suspected major LLOs in *ebs3-1 bri1-9*, *alg3-T2 bri1-9*, or transgenic *gEBS4 ebs3-1 bri1-9* line. Rectangles denote the two GlcNAc residues and circles represent Man residues with black circles indicating α1,6-linked Man residues. (*B*) Images of 5-wk-old soil-grown transgenic *ebs3-1 bri1-9* mutant containing *pPZP212*, a *gEBS3*, or *gEBS4* genomic transgene. (*C*) Immunoblot analysis of the bri1-9 abundance. Numbers in *B* and *C* indicate independent transgenic lines. (*D*) Images of 5-wk-old soil-grown mutants of *ebs3-1 bri1-9*, *bri1-9*, and *alg3-T2 bri1-9*. (*E*) Immunoblot analysis of PDI and bri1-9. For *C* and *E*, equal amounts of total proteins extracted in 2× SDS buffer from 4-wk-old leaves were treated with or without 10 μM Kif, separated by SDS/PAGE, and analyzed by immunoblot with anti-PDI or anti-BRI1 antibody. Coomassie blue staining of RbcS served as a loading control.

2-like protein (SDF2), required for the correct folding of EFR (40), failed to enhance the *bri1-9* dwarfism (Fig. S7) even though the *sdf2-2* mutant was hypersensitive to ER stresses (41), suggesting that the phenotypic enhancement of *bri1-9* by *alg3-T2* is not caused by an abnormal ER stress response but is likely attributable to a stimulatory effect of *alg3-T2* on the bri1-9 ERAD. Indeed, immunoblotting with a BRI1 antibody revealed that whereas *alg3-T2* increases the mobility of bri1-9 because of smaller N-glycans, it decreases the bri1-9 abundance, which is the exactly opposite of what was observed in *ebs3-1* and *ebs4-1* mutants that accumulate larger N-glycan precursors (Fig. 5*E*). Interestingly, the ERAD of bri-9 in *alg3-T2 bri1-9* could still be inhibited by treatment with kifunensine (Kif), a well-known inhibitor of α1,2 mannosidase (42) that prevents ERAD of both bri1-5 and bri1-9 carrying fully assembled N-glycans (19, 20) (Fig. 5*E*), although its inhibitory effect on the bri1-9 ERAD is much weaker in *alg3-T2 bri1-9* than in *bri1-9*, suggesting that the bri1-9 ERAD might require additional Man trimming. Taken together, these results strongly suggested that an exposed α1,6 Man is likely the glycan signal for a plant ERAD process.

Discussion

In this study, we demonstrated that *EBS3* encodes the *Arabidopsis* ortholog of yALG9 that catalyzes the ER luminal addition of two α1,2 Man residues for assembling $Glc_3Man_9GlcNAc_2$ (31). First, *ebs3-1* contains a single-nucleotide change in *At1g16900*, and its *bri1-9* suppressor phenotype was rescued by expression of a genomic *At1g16900* transgene. Second, the predicted At1g16900 protein exhibits the highest sequence homology among all annotated *Arabidopsis* proteins to the yeast ALG9 protein (Fig. S8). The other two *Arabidopsis* proteins showing limited sequence homology are EBS4 and At5g14850 annotated to encode a putative homolog of the yeast PIG-B involved in glycosylphosphatidylinositol biosynthesis (35). Third, the WT At1g16900 was able to complement the growth phenotype of the yeast *Δalg9 wbp1-2* double mutant and the *N*-glycosylation defect of CPY of the *Δalg9* yeast mutant (Fig. 4 *C* and *D*). Consistent with sequence analysis suggesting a crucial catalytic role of the Arg100 residue for several mannosyltransferases (35), our yeast complementation assay showed that the R100W mutation destroys its α1,2 mannosyltransferase activity in yeast cells, suggesting that *ebs3-1* is likely a null mutant. Thus, EBS3 works together with the recently discovered AtALG3 (22, 23) and EBS4 (20) as the three *Arabidopsis* ER-luminal mannosyltransferases to add four more Man residues to Dol-PP-$Man_5GlcNAc_2$ to assemble Dol-PP-$Man_9GlcNAc_2$ that will be triglucosylated before the fully assembled $Glc_3Man_9GlcNAc_2$ can be transferred to nascent polypeptides (Fig. S1).

In yeast, the α1,2 mannosyltransferase ALG9 catalyzes the ER luminal addition of two terminal α1,2 Man residues to create the B- and C-dimannose branches (31), whereas the α1,6 mannosyltransferase ALG12 exhibits high substrate specificity toward Dol-PP-$Man_7GlcNAc_2$ but is very inefficient in adding the second α1,6 Man when the B-branch lacks the terminal α1,2 Man (43) (Fig. S1). Thus, null *alg9* mutations in yeast result in accumulation of Dol-PP-$Man_6GlcNAc_2$ and protein hypoglycosylation because of reduced transfer efficiency of immature glycans by the yeast oligosaccharide transferase (OST) (21, 43). Consistent with our findings that EBS3 is an *Arabidopsis* ortholog of yALG9 and that the R100W mutation is either a null or very severe mutation, our HPLC analyses of LLOs indicated that *ebs3-1 bri1-9* accumulates Dol-PP-$Man_6GlcNAc_2$. Surprisingly, *ebs3-1 bri1-9* also accumulates Dol-PP-$Man_5GlcNAc_2$, the known substrate for ALG3 (22, 23). This is likely caused by feedback inhibition of ALG3 by overaccumulation of its product, Dol-PP-$Man_6GlcNAc_2$, because Dol-PP-$Man_5GlcNAc_2$ was also detected in a yeast *alg9* mutant (21). Despite the glycan-assembly defect, neither the WT BRI1 nor bri1-9 is hypoglycosylated, which is likely attributable to the fact that the *Arabidopsis* OSTs can efficiently transfer truncated glycans from their Dol-PP linker to bri1-9 and other glycoproteins (22, 23), explaining no obvious growth defect of an *ebs3-1 BRI1*$^+$ mutant (Fig. S3*C*).

A crucial decision in ERQC is when to stop futile refolding attempts to divert a terminally misfolded protein from the CNX/CRT cycle to ERAD. A previously popular "mannosidase timer" model posited that the slow α1,2 Man trimming of the B-branch by ERManI generates the ERAD glycan $Man_8GlcNAc_2$ that can be recognized by dedicated ERAD lectins (7). However, recent studies showed that although trimming the B-branch is a necessary ERAD step, the true ERAD signal is an exposed α1,6 Man created by trimming the C-branch (9, 10). In this study, we carried out two genetic experiments that suggested that α1,6 Man-exposed N-glycans likely function as a conserved glycan signal for a plant ERAD process. First, we showed that overexpression of *EBS4* in *ebs3-1 bri1-9* neutralized the suppressive effect of *ebs3-1* on *bri1-9* by promoting bri1-9 ERAD because overexpressed ALG12 in yeast could bypass the requirement of a complete B-branch for adding an α1,6 Man residue (Fig. 5*A*). SF-HPLC coupled with RP-HPLC analyses did detect the presence of a Dol-PP-$Man_7GlcNAc_2$ lacking the B- and C-branch terminal α1,2 Man residues in a *gEBS4 ebs3-1 bri1-9* transgenic mutant (Fig. S4*C*). This unique α1,6 Man-exposing $Man_7GlcNAc_2$ glycan is likely transferred from its Dol-PP linker to bri1-9 in the *gEBS4 ebs3-1 bri1-9* transgenic line because its electromobility on immunoblot is slightly reduced compared with that of bri1-9 in a transgenic *ebs3-1 bri1-9* line carrying an empty vector (Fig. 5*C*). Second, we crossed a T-DNA insertional *alg3-T2* mutation, which is known to create N-glycans carrying a different free α1,6 Man residue (Fig. 5*A*) (22, 23), to *bri1-9* and discovered that the bri1-9 level in *alg3-T2 bri1-9* is lower instead of higher than that in *ebs3-1 bri1-9* and *ebs4-1 bri1-9* despite the N-glycans on bri1-9 carrying fewer Man residues in *alg3-T2* than that in the two *ebs* mutants. Taken together, these results suggested that the glycan signal to mark an ERAD client protein is likely conserved in plants. Given the recent discoveries showing that EFR is misfolded and degraded in the absence of UGGT, CRT3, and other ER proteins/chaperones (13), it will be interesting to determine whether ERAD of incompletely folded EFR also depends on such a conserved N-glycan signal.

Materials and Methods

Plant Materials and Growth Conditions. *Arabidopsis* ecotype Col-0 is the parental line for mutants and transgenic plants except *bri1-9* (Ws-2) for cloning *EBS3* and *bri1-5* (Ws-2) for genetic analysis. The T-DNA mutants of ALG3 (TAIR accession no. SALK_046061) and SDF2 (TAIR accession no. SALK_141321) were obtained from the *Arabidopsis* Biological Resource Center (ABRC) at Ohio State University. Methods for seed sterilization and conditions for plant growth were described previously (44).

Plasmid Construction and Generation of Transgenic Plants. The *p35S-EBS1* and the genomic constructs of *EBS2* and *EBS4* were described previously (18, 20). A 5-kb genomic fragment of *At1g16900*, including 1.5-kb promoter and 500-bp terminator sequences, was PCR-amplified from the BAC clone F17F16, cloned into *pPZP212* (45) to make *pPZP212-gEBS3*, and sequenced to ensure no PCR error. Empty vectors and transgene constructs of *EBS1*, *EBS2*, *EBS3*, and *EBS4* were individually transformed into *bri1-9* or *ebs3-1 bri1-9* mutants by the vacuum infiltration method (46).

Yeast Growth and Complementation Assay. Standard growth medium and conditions were used to grow the wild-type yeast strain SS328, *Δalg9* strain YG414, and *Δalg9 wbp1-2* strain YG415 (21). The ORF of *EBS3* was PCR-amplified from the *At1g16900* cDNA clone U24181 to replace that of the yeast *ALG9* from the *pYEp352-yALG9* expression plasmid to create *pYEp352-EBS3* using the strategy described previously (20). The Stratagene QuikChange XL Site-Directed Mutagenesis kit was used to generate *pYEp352-ebs3-1* from *pYEp352-EBS3* using the primers listed in Table S1. These plasmids were fully sequenced to ensure no PCR error and were individually transformed into YG414 or YG415 via a rapid transformation protocol (47).

Protein Extraction and Immunoblot Analysis. *Arabidopsis* seedlings harvested from agar, soil, or liquid 1/2 Murashige and Skoog (MS) medium supplemented with or without BL (Chemiclones) or Kif (Toronto Research Chemicals) were ground in liquid N_2, dissolved (50 mg seedlings/100 μL) in 2× SDS buffer [0.125 M Tris pH 6.8, 4% (wt/vol) SDS, 20% (vol/vol) glycerol, 0.2 M DTT, 0.02% (wt/vol) bromophenol blue] and boiled for 10 min. After centrifugation, supernatants were used for immunoblot analyses or incubated with or without 1,000 U of Endo Hf in 1× G5 buffer (New England Biolabs) for 1 h at 37 °C. To perform the CHX chase experiment, 3-wk-old seedlings were transferred from 1/2 MS agar plates into 1/2 MS medium containing 180 μM CHX (Sigma), and equal amounts of seedlings were removed at different time points to extract total proteins into 2× SDS sample buffer. After 10 min of boiling, equal amounts of total proteins, equivalent of 5 mg of seedlings, were separated by 7.5% SDS/PAGE and analyzed by immunoblot with anti-BRI1 antibody. To extract yeast proteins, cells of midlog phase grown in a 28 °C shaking incubator were collected by centrifugation, resuspended in 1× extraction buffer [0.3 M sorbitol, 0.1 M NaCl, 5 mM MgCl2, and 10 mM Tris (pH7.4)], lysed by violent vortexing with glass beads, mixed with equal volume of 2× SDS buffer, boiled for 10 min, and centrifuged to collect supernatants. Protein samples of plants or yeast cells were separated on 7% or 10% SDS/PAGE gel, transferred onto Immobilon-P membrane (Millipore), and analyzed by immunoblot with antibodies made against BRI1 (27), PDI (Rose Biotechnology), BiP (SPA-818; Stressgen), maize-CRTs (48), or a monoclonal anti-CPY antibody (10A5; Invitrogen).

Extraction and Analysis of LLOs. The LLOs from *bri1-9*, *bri1-9 ebs3-1*, and *gEBS4 ebs3-1 bri1-9* were extracted, hydrolyzed, pyridylaminated, and analyzed by SF-HPLC and RP-HPLC according to a previously reported protocol (23). The elution positions of PA-labeled oligosaccharides were compared with those of PA-sugar standards purchased from Masuda Chemical Industries.

ACKNOWLEDGMENTS. We thank ABRC for supplying cDNA/BAC clones of *At1g16900* and T-DNA insertional mutant of *ALG3* (TAIR accession no. SALK_046061) and *SDF2* (TAIR accession no. SALK_141321), F. Tax for seeds of *bri1-9* (WS-2) and *bri1-5*, J. Chory for anti-BRI1 antibody, Y. Yin for anti-BES1 antiserum, R. Boston for anti-maize CRT antibody, A. Chang for anti-CPY antibody, M. Aebi for yeast strains and *YEp352-yALG9* plasmid, and members of Li laboratory for stimulating discussion. This work was supported, in part, by National Natural Science Foundation of China Grant 31070246 (to Z.H.), National Institutes of Health Grant GM060519 (to J.L.), and Department of Energy Grant ER15672 (to J.L.).

1. Abu-Qarn M, Eichler J, Sharon N (2008) Not just for Eukarya anymore: Protein glycosylation in Bacteria and Archaea. *Curr Opin Struct Biol* 18:544–550.
2. Kelleher DJ, Gilmore R (2006) An evolving view of the eukaryotic oligosaccharyltransferase. *Glycobiology* 16:47R–62R.
3. Helenius A, Aebi M (2004) Roles of N-linked glycans in the endoplasmic reticulum. *Annu Rev Biochem* 73:1019–1049.
4. Molinari M (2007) N-glycan structure dictates extension of protein folding or onset of disposal. *Nat Chem Biol* 3:313–320.
5. Caramelo JJ, Parodi AJ (2007) How sugars convey information on protein conformation in the endoplasmic reticulum. *Semin Cell Dev Biol* 18:732–742.
6. Caramelo JJ, Parodi AJ (2008) Getting in and out from calnexin/calreticulin cycles. *J Biol Chem* 283:10221–10225.
7. Lederkremer GZ, Glickman MH (2005) A window of opportunity: Timing protein degradation by trimming of sugars and ubiquitins. *Trends Biochem Sci* 30:297–303.
8. Vembar SS, Brodsky JL (2008) One step at a time: Endoplasmic reticulum-associated degradation. *Nat Rev Mol Cell Biol* 9:944–957.
9. Clerc S, et al. (2009) Htm1 protein generates the N-glycan signal for glycoprotein degradation in the endoplasmic reticulum. *J Cell Biol* 184:159–172.
10. Quan EM, et al. (2008) Defining the glycan destruction signal for endoplasmic reticulum-associated degradation. *Mol Cell* 32:870–877.
11. Ceriotti A, Roberts LM (2006) Endoplasmic reticulum-associated protein degradation in plant cells. *The Plant Endoplasmic Reticulum*, ed Robinson DG (Springer, Heidelberg), pp 75–98.
12. Vitale A, Boston RS (2008) Endoplasmic reticulum quality control and the unfolded protein response: Insights from plants. *Traffic* 9:1581–1588.
13. Saijo Y (2010) ER quality control of immune receptors and regulators in plants. *Cell Microbiol* 12:716–724.
14. Li J, Chory J (1997) A putative leucine-rich repeat receptor kinase involved in brassinosteroid signal transduction. *Cell* 90:929–938.
15. Kinoshita T, et al. (2005) Binding of brassinosteroids to the extracellular domain of plant receptor kinase BRI1. *Nature* 433:167–171.
16. Zipfel C, et al. (2006) Perception of the bacterial PAMP EF-Tu by the receptor EFR restricts *Agrobacterium*-mediated transformation. *Cell* 125:749–760.
17. Jin H, Yan Z, Nam KH, Li J (2007) Allele-specific suppression of a defective brassinosteroid receptor reveals a physiological role of UGGT in ER quality control. *Mol Cell* 26:821–830.
18. Jin H, Hong Z, Su W, Li J (2009) A plant-specific calreticulin is a key retention factor for a defective brassinosteroid receptor in the endoplasmic reticulum. *Proc Natl Acad Sci USA* 106:13612–13617.
19. Hong Z, Jin H, Tzfira T, Li J (2008) Multiple mechanism-mediated retention of a defective brassinosteroid receptor in the endoplasmic reticulum of *Arabidopsis*. *Plant Cell* 20:3418–3429.
20. Hong Z, et al. (2009) Mutations of an alpha1,6 mannosyltransferase inhibit endoplasmic reticulum-associated degradation of defective brassinosteroid receptors in *Arabidopsis*. *Plant Cell* 21:3792–3802.
21. Burda P, et al. (1996) Stepwise assembly of the lipid-linked oligosaccharide in the endoplasmic reticulum of *Saccharomyces cerevisiae:* Identification of the *ALG9* gene encoding a putative mannosyl transferase. *Proc Natl Acad Sci USA* 93:7160–7165.
22. Henquet M, et al. (2008) Identification of the gene encoding the alpha1,3-mannosyltransferase (ALG3) in *Arabidopsis* and characterization of downstream n-glycan processing. *Plant Cell* 20:1652–1664.
23. Kajiura H, Seki T, Fujiyama K (2010) *Arabidopsis thaliana ALG3* mutant synthesizes immature oligosaccharides in the ER and accumulates unique N-glycans. *Glycobiology* 20:736–751.
24. Su W, Liu Y, Xia Y, Hong Z, Li J (2011) Conserved endoplasmic reticulum-associated degradation system to eliminate mutated receptor-like kinases in *Arabidopsis*. *Proc Natl Acad Sci USA* 108:870–875.
25. Maley F, Trimble RB, Tarentino AL, Plummer TH, Jr. (1989) Characterization of glycoproteins and their associated oligosaccharides through the use of endoglycosidases. *Anal Biochem* 180:195–204.
26. Clouse SD, Langford M, McMorris TC (1996) A brassinosteroid-insensitive mutant in *Arabidopsis thaliana* exhibits multiple defects in growth and development. *Plant Physiol* 111:671–678.
27. Mora-García S, et al. (2004) Nuclear protein phosphatases with Kelch-repeat domains modulate the response to brassinosteroids in *Arabidopsis*. *Genes Dev* 18:448–460.
28. Houston NL, et al. (2005) Phylogenetic analyses identify 10 classes of the protein disulfide isomerase family in plants, including single-domain protein disulfide isomerase-related proteins. *Plant Physiol* 137:762–778.
29. Sung DY, Vierling E, Guy CL (2001) Comprehensive expression profile analysis of the Arabidopsis Hsp70 gene family. *Plant Physiol* 126:789–800.
30. Persson S, et al. (2003) Phylogenetic analyses and expression studies reveal two distinct groups of calreticulin isoforms in higher plants. *Plant Physiol* 133:1385–1396.
31. Frank CG, Aebi M (2005) ALG9 mannosyltransferase is involved in two different steps of lipid-linked oligosaccharide biosynthesis. *Glycobiology* 15:1156–1163.
32. Frank CG, et al. (2004) Identification and functional analysis of a defect in the human *ALG9* gene: Definition of congenital disorder of glycosylation type *IL*. *Am J Hum Genet* 75:146–150.
33. Jakob CA, Burda P, Roth J, Aebi M (1998) Degradation of misfolded endoplasmic reticulum glycoproteins in *Saccharomyces cerevisiae* is determined by a specific oligosaccharide structure. *J Cell Biol* 142:1223–1233.
34. Weinstein M, et al. (2005) CDG-IL: An infant with a novel mutation in the *ALG9* gene and additional phenotypic features. *Am J Med Genet A* 136:194–197.
35. Oriol R, Martinez-Duncker I, Chantret I, Mollicone R, Codogno P (2002) Common origin and evolution of glycosyltransferases using Dol-P-monosaccharides as donor substrate. *Mol Biol Evol* 19:1451–1463.
36. Kostova Z, Wolf DH (2005) Importance of carbohydrate positioning in the recognition of mutated CPY for ER-associated degradation. *J Cell Sci* 118:1485–1492.
37. Kanehara K, Kawaguchi S, Ng DT (2007) The EDEM and Yos9p families of lectin-like ERAD factors. *Semin Cell Dev Biol* 18:743–750.
38. Burda P, Jakob CA, Beinhauer J, Hegemann JH, Aebi M (1999) Ordered assembly of the asymmetrically branched lipid-linked oligosaccharide in the endoplasmic reticulum is ensured by the substrate specificity of the individual glycosyltransferases. *Glycobiology* 9:617–625.
39. Alonso JM, et al. (2003) Genome-wide insertional mutagenesis of *Arabidopsis thaliana*. *Science* 301:653–657.
40. Nekrasov V, et al. (2009) Control of the pattern-recognition receptor EFR by an ER protein complex in plant immunity. *EMBO J* 28:3428–3438.
41. Schott A, et al. (2010) *Arabidopsis* stromal-derived Factor2 (SDF2) is a crucial target of the unfolded protein response in the endoplasmic reticulum. *J Biol Chem* 285:18113–18121.
42. Tokunaga F, Brostrom C, Koide T, Arvan P (2000) Endoplasmic reticulum (ER)-associated degradation of misfolded N-linked glycoproteins is suppressed upon inhibition of ER mannosidase I. *J Biol Chem* 275:40757–40764.
43. Cipollo JF, Trimble RB (2000) The accumulation of Man(6)GlcNAc(2)-PP-dolichol in the *Saccharomyces cerevisiae Deltaalg9* mutant reveals a regulatory role for the Alg3p alpha1,3-Man middle-arm addition in downstream oligosaccharide-lipid and glycoprotein glycan processing. *J Biol Chem* 275:4267–4277.
44. Li J, Nam KH, Vafeados D, Chory J (2001) *BIN2*, a new brassinosteroid-insensitive locus in Arabidopsis. *Plant Physiol* 127:14–22.
45. Hajdukiewicz P, Svab Z, Maliga P (1994) The small, versatile pPZP family of *Agrobacterium* binary vectors for plant transformation. *Plant Mol Biol* 25:989–994.
46. Bechtold N, Pelletier G (1998) *In planta Agrobacterium*-mediated transformation of adult *Arabidopsis thaliana* plants by vacuum infiltration. *Methods Mol Biol* 82:259–266.
47. Gietz RD, Woods RA (2002) Transformation of yeast by lithium acetate/single-stranded carrier DNA/polyethylene glycol method. *Methods Enzymol* 350:87–96.
48. Pagny S, et al. (2000) Protein recycling from the Golgi apparatus to the endoplasmic reticulum in plants and its minor contribution to calreticulin retention. *Plant Cell* 12:739–756.